PROCEEDINGS OF SPIE

GaN/AlGaN avalanche photodiode detectors for high performance ultraviolet sensing applications

Sood, Ashok, Zeller, John, Ghuman, Parminder, Babu, Sachidananda, Dupuis, Russell

SPIE.

GaN/AlGaN Avalanche Photodiode Detectors for High Performance Ultraviolet Sensing Applications

Ashok K. Sood and **John W. Zeller**

Magnolia Optical Technologies, Inc., 52-B Cummings Park, Suite 314, Woburn, MA 01801

Parminder Ghuman and **Sachidananda Babu**

NASA Earth Science Technology Office, Greenbelt, MD 20771

Russell D. Dupuis

School of Electrical & Computer Engineering, Georgia Institute of Technology,
Atlanta, GA 30332

ABSTRACT

The shorter wavelengths of the ultraviolet (UV) band enable detectors to operate with increased spatial resolution, variable pixel sizes, and large format arrays, benefitting a variety of NASA, defense, and commercial applications. $Al_xGa_{1-x}N$ semiconductor alloys, which have attracted much interest for detection in the UV spectral region, have been shown to enable high optical gains, high sensitivities with the potential for single photon detection, and low dark current performance in ultraviolet avalanche photodiodes (UV-APDs). We are developing GaN/AlGaN UV-APDs with large pixel sizes that demonstrate consistent and uniform device performance and operation. These UV-APDs are fabricated through high quality metal organic chemical vapor deposition (MOCVD) growth on lattice-matched, low dislocation density GaN substrates with optimized material growth and doping parameters. The use of these low defect density substrates is a critical element to realizing highly sensitive UV-APDs and arrays with suppressed dark current under high electric fields. Optical gains greater than 5×10^6 with enhanced quantum efficiencies over the 350-400 nm spectral range have been demonstrated, enabled by a strong avalanche multiplication process. Furthermore, we are developing 6×6 arrays of devices to test high gain UV-APD array performance at ~355 nm. These variable-area GaN/AlGaN UV-APD detectors and arrays enable advanced sensing performance over UV bands of interest with high resolution detection for NASA Earth Science applications.

Keywords: Avalanche photodiodes, ultraviolet, GaN, AlGaN, MOCVD, high gain, thin films, sensor arrays

1. INTRODUCTION

For many space and defense applications, spectral information beyond that which can be provided by conventional visible sensors are desired. Detection of shorter wavelengths over the UV spectrum provides greater spatial resolutions, which allows for various pixel sizes and larger formats [1-3]. UV sensing applications include chemical and biological detection of surface residues and bio-aerosol agents, machine vision, and space research for NASA and defense applications [4].

Avalanche photodiodes (APDs) based on AlGaN semiconductor alloys offer advantages of high optical gains, high sensitivities, low dark currents, and chemical and thermal stability for many demanding applications [5]. Development of arrays of APD pixels as small as 4 μm is achievable with this material technology [1]. Since the operating wavelength range of $Al_xGa_{1-x}N$ APDs is adjustable by controlling the Al concentration in the material, these devices enable detection of photons over large portions of the UV spectrum.

Growth of AlGaN material for high gain ultraviolet avalanche photodiode (UV-APD) arrays has traditionally been restricted to the use of lattice-mismatched substrates such as SiC and sapphire due to the lack of availability of native III-N substrates [6]. However, the lattice mismatch and differences in the thermal expansion coefficients between such foreign substrates can lead to strain-induced defects, resulting in high leakage current and premature microplasma breakdown prior to reaching avalanche breakdown [7]. To improve the growth process, low dislocation density *n*-type GaN substrates have been employed to successfully improve the crystalline and structural quality of the epitaxial layers.

Figure 1. High-temperature MOCVD system with close-coupled showerhead for UV-APD development [5].

To advance the technology for UV detection, Magnolia in collaboration with the Georgia Institute of Technology is developing GaN/AlGaN UV-APDs single devices and arrays on lattice-matched GaN substrates for high-sensitivity UV sensing and imaging using metalorganic chemical vapor deposition (MOCVD). Figure 1 shows the upgraded AIXTRON MOCVD growth reactor and close-coupled showerhead at Georgia Tech, which provides uniformity control for growth of high quality GaN and AlGaN material with doping [5]. These high-performance detectors and arrays with improved frontside-illuminated performance enable high resolution detection and imaging at the ~355 nm wavelength for NASA Earth Science applications.

2. GAN/ALGAN UV-APD DEVICE FABRICATION AND MATERIAL STRUCTURES

Epitaxial layers of GaN *p-i-n* and *p-i-p-i-n* UV-APDs structures were grown on GaN substrates as well as on GaN/sapphire templates in an AIXTRON MOCVD growth reactor at Georgia Tech (shown in Figure 1) with a close-coupled showerhead that provides uniformity control for growth of high quality GaN and AlGaN material with doping for UV-APD applications [8]. The lattice-matched substrates are composed of *n*-type Si-doped bulk GaN having threading dislocation densities lower than 5×10^4 cm^{-2}. Figure 2 shows a schematic cross-sectional structure of the epitaxial layers of a GaN *p-i-n* APD. The *p-i-n* APD structure consists of a 1.0 μm thick *n*-GaN:Si layer ($n \sim 8 \times 10^{18}$ cm^{-3}, $\mu_n \sim 223$ cm^2/V·s, $\rho \sim 0.003$ Ω-cm), an 0.2 μm thick unintentionally doped *u*-GaN layer, an 0.1-μm thick *p*-GaN:Mg layer ($p \sim 6 \times 10^{17}$ cm^{-3}, $\mu_p \sim 15$ cm^2/V·s, $\rho \sim 0.727$ Ω-cm), and a 20 nm thick p^+-GaN:Mg layer with cut-off wavelength of 365 nm.

GaN *p-i-p-i-n* separate absorption and multiplication (SAM) UV-APDs with large detection areas grown by MOCVD have also been fabricated on bulk GaN substrates having low defect densities. For further enhancement of the responsivity and external quantum efficiency (EQE) of the front-illuminated UV-APDs, a higher-Al-composition *p*-type Al$_x$Ga$_{1-x}$N layer or thicker absorption layer may be used. For the frontside-illuminated electron-initiated multiplication process, a *p*-type Al$_{0.05}$Ga$_{0.95}$N:Mg layer was introduced as a window layer instead of a *p*-GaN:Mg layer to reduce the UV-light absorption in the *p*-type contact layer. Figure 3(a) shows the schematic cross-sectional structure for the fabricated GaN/AlGaN *p-i-p-i-n* UV-APDs.

The GaN/AlGaN UV-APDs have been fabricated with mesa sizes ranging from 2,000 μm^2 to 10,000 μm^2 using low damage inductively coupled plasma reactive-ion etching (ICP-RIE). A top-view scanning electron microscopy (SEM) image of the physical layout showing the metal contact pads and circular mesa is shown in Figure 3(b) [9,10]. Ti/Al/Ti/Au and Ni/Ag/Ni/Au metal stacks were evaporated and annealed on the *n*-type and *p*-type contact layers, respectively. To suppress mesa sidewall leakage current and prevent premature breakdown under high reverse bias, a SiO$_2$ passivation layer was deposited using plasma-enhanced chemical vapor deposition (PECVD) with accessing via holes opened by subsequent ICP-RIE. Finally, thick Ti/Au metal stacks were evaporated for metal interconnects and bonding pads.
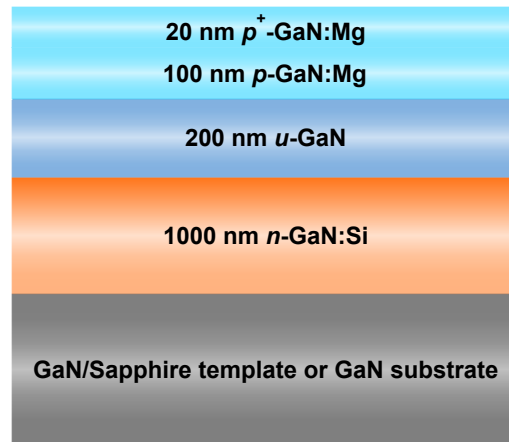
Figure 2. Schematic diagram of epitaxial layers of GaN p-i-n APDs structure.
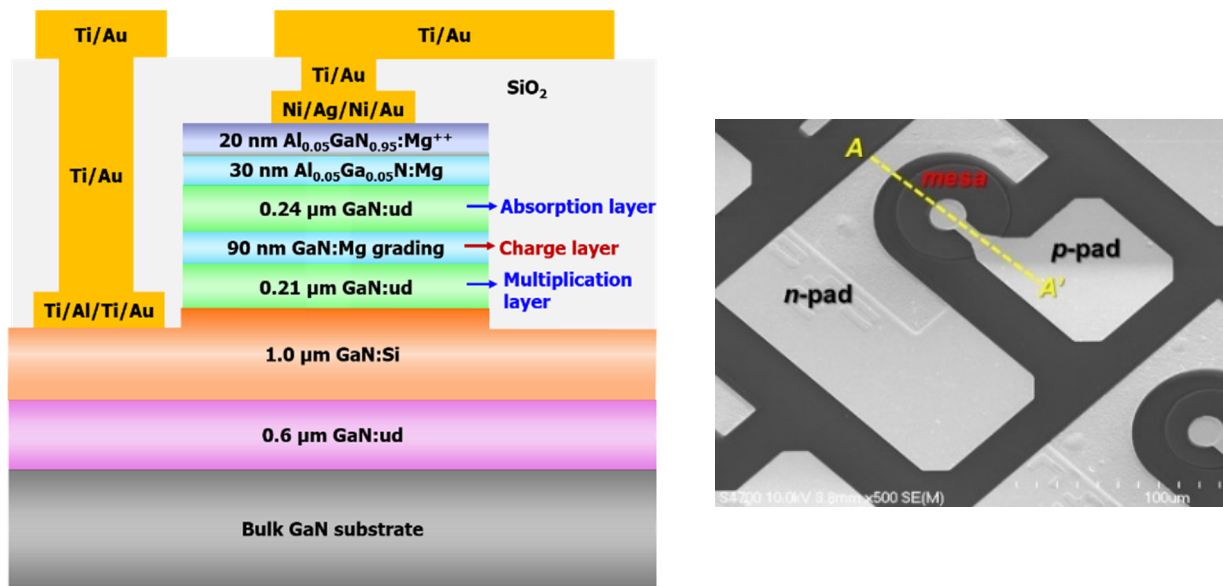

Figure 3. (a) Schematic cross-sectional structure of a top-illuminated GaN/AlGaN p-i-p-i-n UV-APD with AlGaN:Mg p-type window grown on a bulk GaN substrate [9]. (b) SEM image showing top view of APD physical layout [10].

3. GAN/ALGAN UV-APD MATERIAL CHARACTERIZATION

In order to examine the surface morphology and crystal quality of the epitaxial layer structure, characterization techniques including Nomarski optical microscopy, atomic-force microscopy (AFM), X-ray diffraction (XRD), and secondary ion mass spectrometry (SIMS) have been utilized. The AlN mole fractions in the $Al_xGa_{1-x}N$ epitaxial layers were determined by XRD measurements. In addition, Hall-effect measurements at 300 K were used to measure the electrical properties of p-$Al_{0.05}Ga_{0.95}N$:Mg and n-GaN:Si layers.

3.1 UV-APD surface morphology

The surface morphology of UV-APD epitaxial layers and complete GaN UV-APD device structures were studied by Nomarski differential phase-contrast optical microscopy as shown in Figure 4. Likewise, Figure 5 depicts the microscopic surface morphologies measured by atomic-force microscopy (AFM) of the n- and p-type doped calibration layers grown on GaN/sapphire template substrates.
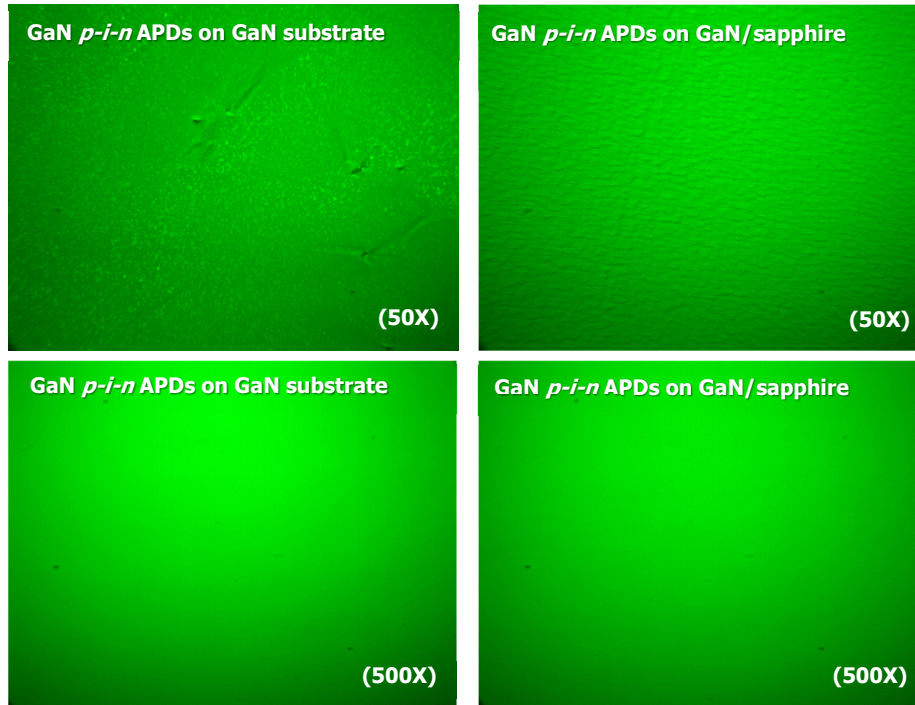
Figure 4. Nomarski phase-contrast optical microscope images of the surface of the GaN *p-i-n* APD wafers. The texture in the 50X images are due to the roughness of the backside of the substrate.
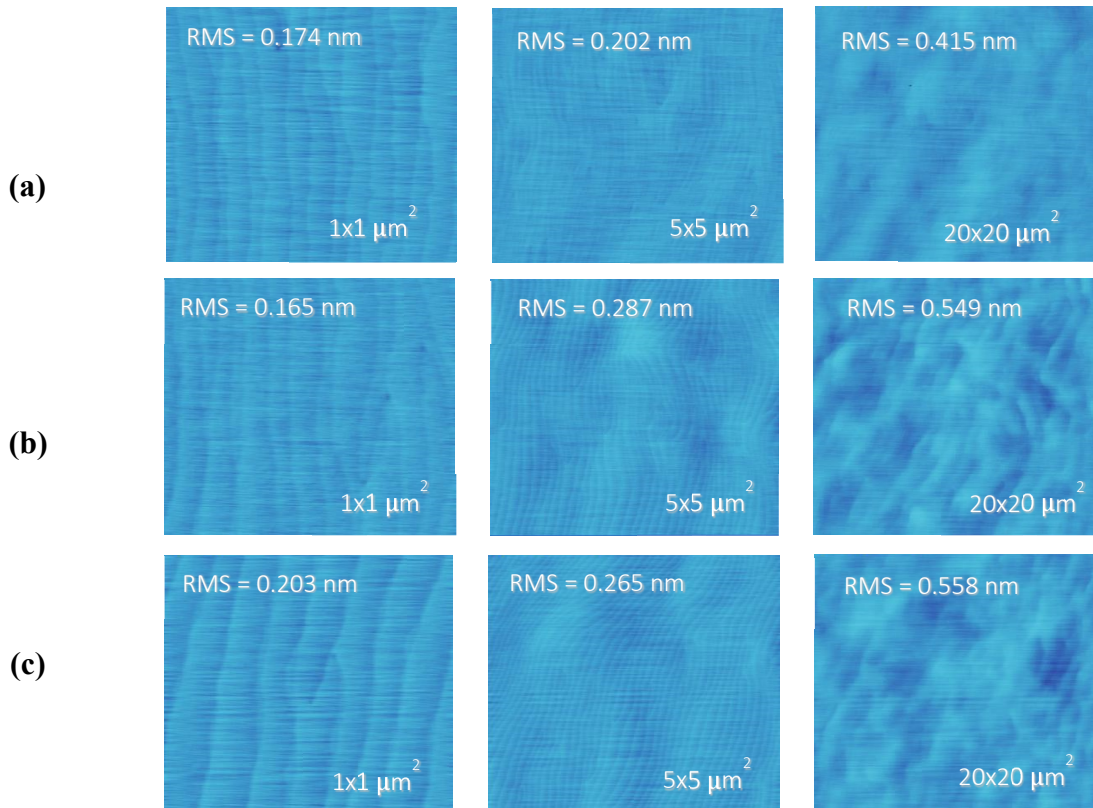

Figure 5. AFM microscopic surface morphology of (a) *n*-GaN:Si layer; (b) *p*-GaN:Mg layer; and (c) *p*-GaN:Mg with *p*⁺-GaN:Mg layer structures grown on *u*-GaN/sapphire templates; with 1×1 μm² scan; 5×5 μm² scan; and 20×20 μm² scan sizes.

3.2 UV-APD dopant profile

Secondary ion mass spectrometry (SIMS) was employed to confirm the Si and Mg doping profiles of the GaN *p-i-n* APDs grown on GaN/sapphire templates as well as the low background impurity concentrations and epitaxial layer thicknesses. As shown in Figure 6, the doping levels of [Si] and [Mg] for the *n*- and *p*-layers are at targeted concentrations of [S] $\sim 8.5 \times 10^{18}$ cm^{-3} and [Mg] $\sim 2 \times 10^{19}$ cm^{-3}, respectively.
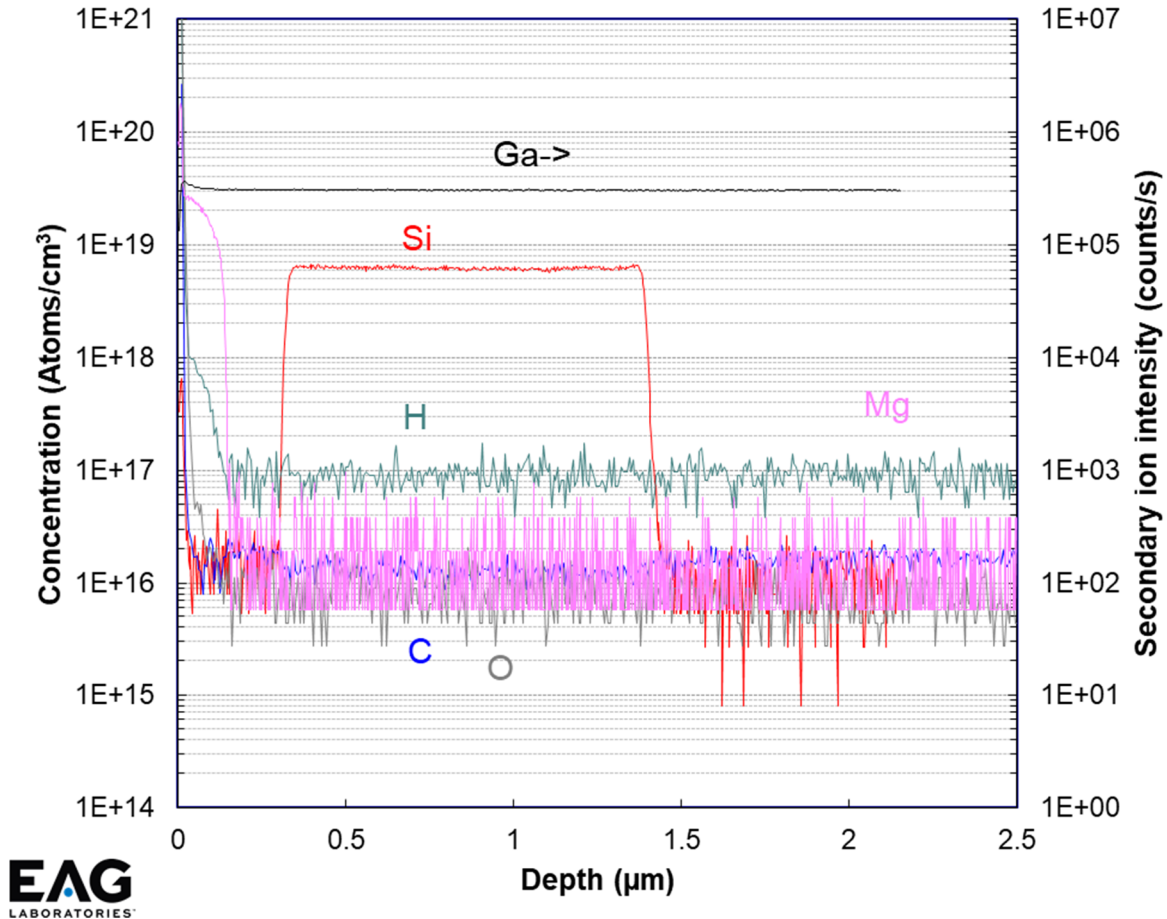

Figure 6. Secondary ion mass spectrometry (SIMS) distribution profiles of silicon (Si), magnesium (Mg), gallium (Ga), carbon (C), hydrogen (H), and oxygen (O) for *p-i-n* GaN UV-APD structure on *u*-GaN/sapphire template.

X-ray diffraction (XRD) was utilized for the characterization of the quality of the crystalline structure of the epitaxial APD layers grown on GaN/sapphire templates and GaN substrates. X-ray rocking curves results of the GaN *p-i-n* APD wafers show full-width at half maximum (FWHM) values of 237 and 304 for (002) and (102), respectively, on GaN/sapphire templates and FWHM values of 74 and 55 for (002) and (102), respectively, on GaN bulk substrates.

Hall-effect characterization at 300 K was also used for measurement of the electrical properties of the doped layers, including the free-carrier concentration and resistivity, on samples having 1×1 cm^2 size. Indium bumps and metal deposition of Ni/Ag/Ni/Au (after chemical preparation) were used as contact points for the *n*- and *p*-type doped layers, respectively.

4. GAN/ALGAN UV-APD ELECTRO-OPTICAL PERFORMANCE

4.1 I-V and gain characteristics

The current-voltage (I-V) and gain characteristics of the GaN/AlGaN UV-APDs were measured using a Keithley Model 4200 semiconductor characterization system under dark conditions and UV illumination with peak wavelength of 340 nm. The dark current density, photocurrent density, and calculated avalanche gain for a UV-APD having 75×75 μm^2 mesa size (detection area of 5,625 μm^2) are shown in Figure 7 [11].
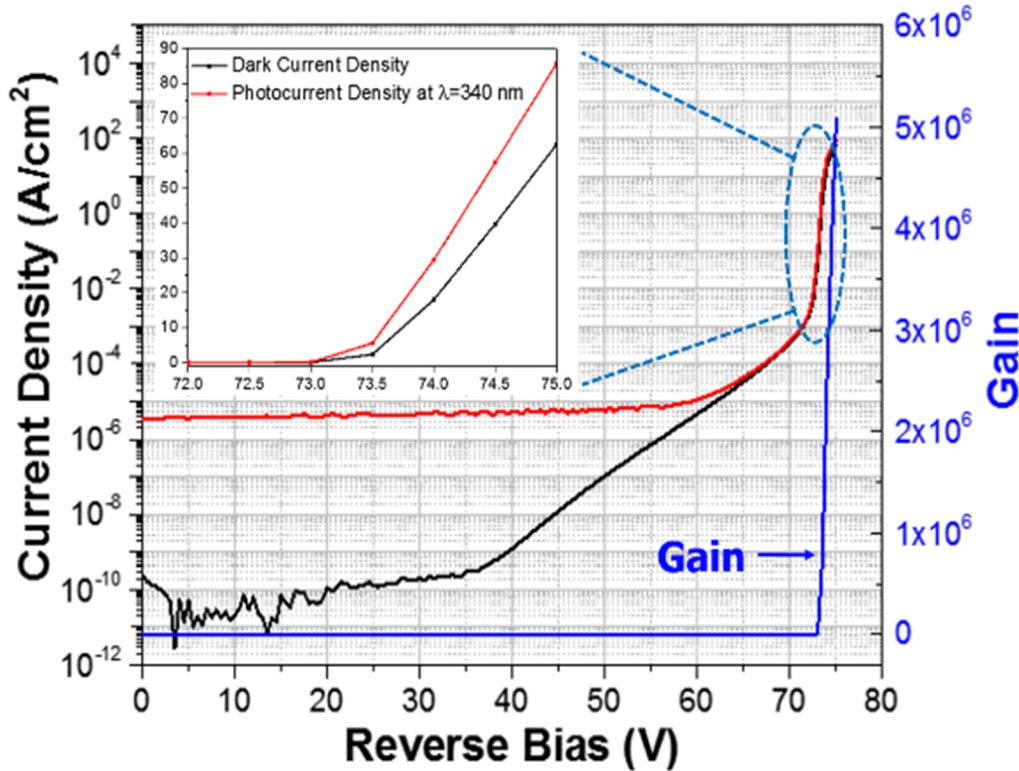

Figure 7. Reverse bias *I-V* and avalanche gain characteristics of GaN/AlGaN UV-APD with 75×75 μm^2 mesa size under dark conditions and UV illumination with peak wavelength of 340 nm [11].

Under dark conditions, the UV-APD with SAM regions exhibited a low leakage current of $\sim 5.6 \times 10^{-14}$ A, corresponding to a dark current density of below 1.0×10^{-9} A/cm^2 up to a reverse bias of 40 V. The low dark current density shows that the concentration of defects in this structure is quite low. The dark current then monotonically increased until reaching the onset point of breakdown voltage. Under UV illumination at 340 nm, this UV-APD showed a photocurrent density of 5.6×10^{-6} A/cm^2, which remained relatively constant and around four orders of magnitude higher that the dark current density up to a reverse bias of ~ 40 V. As the magnitude of the reverse bias increased further, the behavior of the photocurrent density exhibited a similar trend to that of the dark current density.

The avalanche gain of the UV-APD plotted in Figure 7 is 7.8×10^3 at the onset point of voltage breakdown (~ 73 V). (This experimentally measured onset point is ~ 23 V lower than previously achieved with GaN/AlGaN *p-i-n* APDs and is in good agreement with simulated results [1,4].) At this point the gain is seen to rise exponentially corresponding to the sharp rise in photocurrent due to the avalanche multiplication process, rising above 5×10^6 at a reverse bias of 75 V.

This sharp increase in the avalanche gain above the onset point of breakdown indicates that these fabricated UV-APD devices experience a strong avalanche multiplication process. As before, no microplasma breakdown or edge breakdown due to sidewall damage was observed, attributed to the low damage etching process and high-quality dielectric passivation utilized for the UV-APD devices. In addition, the increased maximum avalanche gain and reduced breakdown voltage of the UV-APDs suggest that photogenerated electrons may be promoted to migrate toward the multiplication region by increasing the doping level of the charge layer through impact ionization.

4.2 UV-APD spectral response

The bias-dependent spectral response of a GaN/AlGaN UV-APD with detector mesa size of 75×75 µm^2 was measured under frontside-illumination with an Oriel xenon lamp attached to a Cornerstone 260 monochromator/chopper system and lock-in amplifier. The zero-biased photocurrent exhibits a peak responsivity of 42.5 mA/W at 366 nm, corresponding to an EQE of 14% with an absorption edge at 390 nm, as shown in Figure 8 [11].

It is noted that at a reverse bias of 70 V, the peak responsivity increases to 320 mA/W at 376 nm. In addition, with increasing reverse bias the peak absorption wavelength shifts slightly from 366 nm to 376 nm due to the Franz-Keldysh effect. Detection at the ~355 nm wavelength is achieved with higher concentrations of Al in AlGaN devices, resulting in a blueshift of the absorption peak to this wavelength.
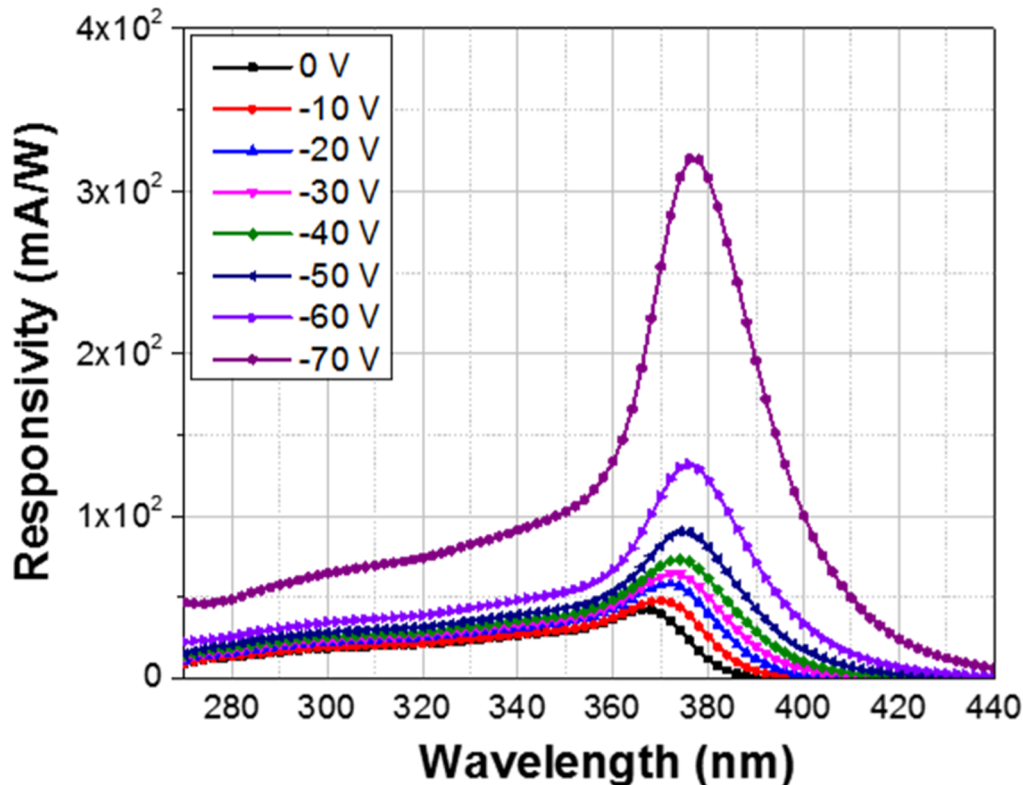

Figure 8. Reverse-voltage-dependent spectral response of GaN/AlGaN UV-APD with mesa size of 75×75 µm^2 [11].

4.3 Further electro-optical measurements

Shown in Figure 9 is the optical transmission vs. cut-off wavelength for the GaN *p-i-n* APD wafers grown on GaN/sapphire templates and GaN substrates at $\lambda \approx 367$ nm and $\lambda \approx 376$ nm, respectively. The measured absorption spectrum cut-off wavelength for the APD structures grown on the free-standing GaN substrates is affected by much larger total thickness of the substrate due to the absorption in the substrate resulting from high *n*-type doping levels and other impurities.

Transmission line measurements (TLM) were also used to investigate the electrical properties of the *n*-GaN and *p*-GaN epitaxial layers. The measured *I-V* curves plotted in Figure 10 show good linearity without a noticeable Schottky barrier, indicating that the contacts between the metal pads and the semiconductor layer have good ohmic characteristics. In addition, the different *I-V* results for the different 60 µm diameter UV-APD devices tested are seen to be quite consistent. It seen that the dark current of a single UV-APD increases until the onset of impact ionization (~67 V), at which point avalanche breakdown starts to occur. Beyond this voltage, the dark current density increases sharply with reverse bias as expected.
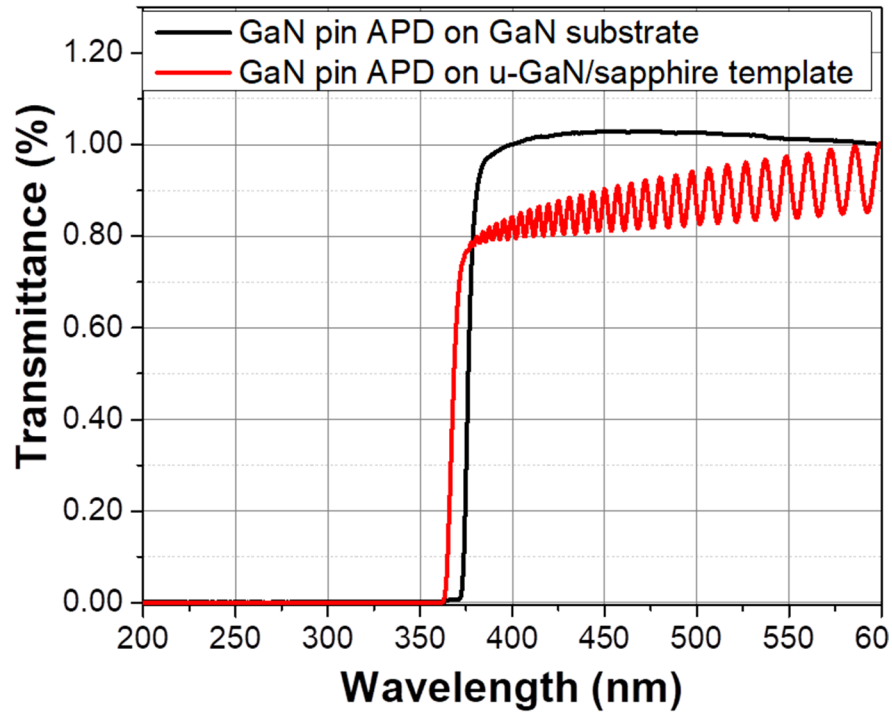
Figure 9. Optical transmission results of GaN *p-i-n* APD wafers grown on GaN/sapphire template and GaN substrate. The absorption cut-off wavelength for the APD structure grown on the GaN substrate is affected by absorption in GaN substrate.
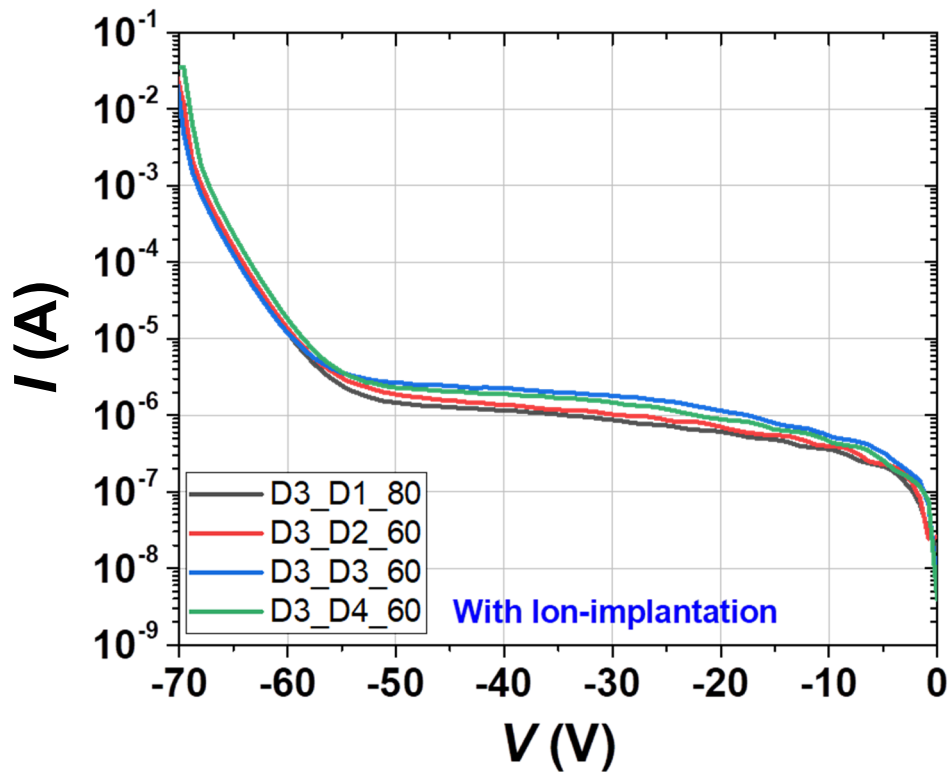

Figure 10. Reverse-bias *I-V* results of 60 μm diameter GaN *p-i-n* UV-APDs grown on GaN substrates.

5. DEVELOPMENT OF 6×6 UV-APD ARRAYS

We are currently working towards the development of 6×6 arrays of GaN UV-APDs with 60 µm unit cells. A set of optical lithography masks has been developed for fabrication, testing, and demonstration of the 6×6 arrays of frontside-illuminated GaN APDs. The mask set used is based upon previous masks for the 4×4 arrays that includes various process control elements for testing ohmic contacts and individual APDs with various areas in addition to the 6×6 arrays. Successful demonstration of 6×6 arrays will enable subsequent development of larger arrays of the UV-APDs. Our goal is to demonstrate high gain UV-APD arrays with peak performance at 355 nm.

A top view of the device layout of the 6×6 arrays is given in Figure 11, showing the overall layout for the wire bonding, packaging, and testing of the 6×6 GaN APD arrays. The ceramic multiple-lead packages to be utilized for testing of the arrays are shown in Figure 12.
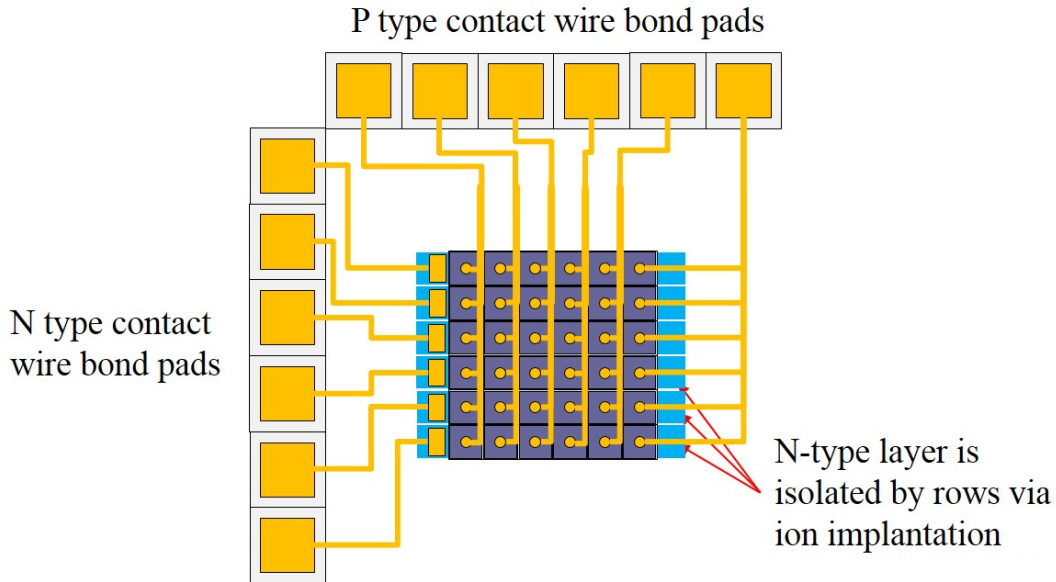

Figure 11. Overall device layout for 6×6 GaN APD arrays, including individual APD test diodes and contact testing patterns.
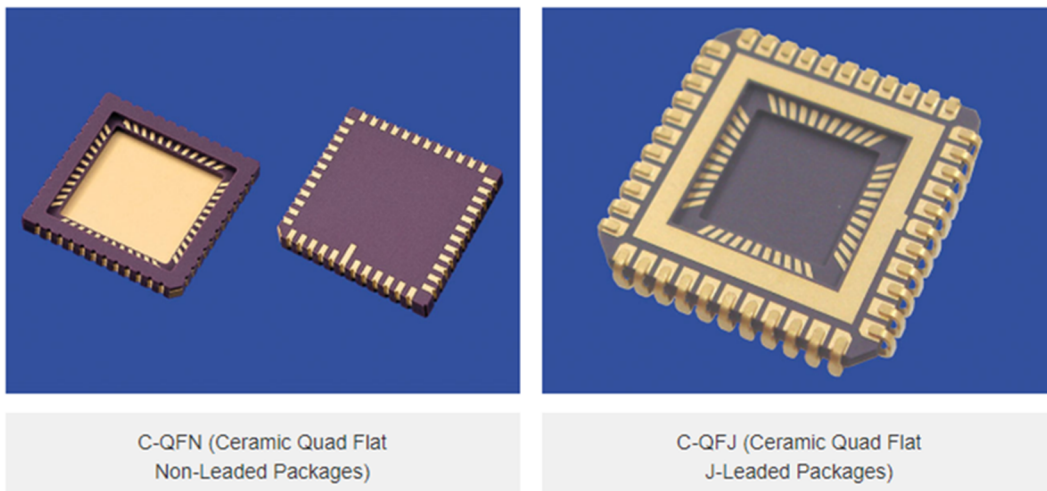

Figure 12. Photographs of ceramic packages to be used for testing of the 6×6 GaN UV-APD arrays.

6. SUMMARY AND CONCLUSIONS

The high gain frontside-illuminated GaN AlGaN detectors and arrays developed on low defect density GaN substrates are advancing the state-of-the-art to provide enhanced capabilities for UV detection, particularly at the ~355 nm wavelength. MOCVD epitaxial growth of AlGaN UV-APDs on native GaN substrates has enabled suppressed microplasma breakdown, providing low dark current densities with comparatively high photocurrents and responsivities over the UV spectrum. In addition, superior gain properties with avalanche gains greater than 5×10^6 and reductions in the breakdown voltage, made possible by the low dislocation substrates have been achieved through impact ionization engineering. Furthermore, we are now developing 6×6 GaN UV-APD arrays to demonstrate high gain performance at ~355 nm. These improvements in GaN/AlGaN APD performance and reliability towards the development and successful implementation of robust, highly sensitive, high performance UV-APD detector arrays to benefit future advanced NASA Earth Science applications.

REFERENCES

[1] A. K. Sood, J. W. Zeller, R. E. Welser, Y. R. Puri, R. D. Dupuis, M.-H. Ji, J. Kim, T. Detchprohm, J. Lewis, and N. K. Dhar, "Development of GaN/AlGaN UVAPDs for ultraviolet sensor applications," Int. J. Phys. Appl. 7(1), 49-58 (2015).

[2] M. B. Reine, A. Hairston, P. Lamarre, K. K. Wong, S. P. Tobin, A. K. Sood, C. Cooke, M. Pophristic, S. Guo, B. Peres, R. Singh, C. R. Eddy, Jr., U. Chowdhury, M. M. Wong, R. D. Dupuis, T. Li, and S. P. DenBaars, "Solar blind AlGaN 256x256 pin detectors and focal plane arrays," Proc. SPIE 6121, 61210R (2006).

[3] A. K. Sood, R. A. Richwine, Y. R. Puri, N. K. Dhar, D. L. Polla, and P. S. Wijewarnasuriya, "Multispectral EO/IR sensor model for evaluating UV, visible, SWIR, MWIR and LWIR system performance," Proc. SPIE 7300, 73000H (2009).

[4] M.-H. Ji, J. Kim, T. Detchprohm, R. D. Dupuis, A. K. Sood, N. K. Dhar, and J. Lewis, "Uniform and reliable GaN pin ultraviolet avalanche photodiode arrays," IEEE Photon. Tech. Lett. 28(19), 2015-2018 (2016).

[5] A. K. Sood, J. W. Zeller, R. E. Welser, Y. R. Puri, R. D. Dupuis, M.-H. Ji, J. Kim, T. Detchprohm, N. K. Dhar, J. S. Lewis, and R. L. Peters, "Development of high gain avalanche photodiodes for UV imaging applications," Proc. SPIE 9609, 96090X (2015).

[6] Q. Zhou, D. C. McIntosh, Z. Lu, J. C. Campbell, A. V. Sampath, H. Shen, and M. Wraback, "GaN/SiC avalanche photodiodes," Appl. Phys. Lett. 99, 131110 (2011).

[7] J. Kim, M.-H. Ji, T. Detchprohm, J.-H. Ryou, R. D. Dupuis, A. K. Sood, and N. K. Dhar, "$Al_xGa_{1-x}N$ ultraviolet avalanche photodiodes with avalanche gain greater than 10^5," IEEE Photon. Tech. Lett. 27(6), 642-645 (2015).

[8] A. K. Sood, J. W. Zeller, Y. R. Puri, R. D. Dupuis, T. Detchprohm, M.-H. Ji, S.-C. Shen, S. Babu, N. K. Dhar, and P. Wijewarnasuriya, "Development of high gain GaN/AlGaN avalanche photodiode arrays for UV detection and imaging applications," Int. J. Engr. Res. Tech. 10(2), 129-150 (2017).

[9] M.-H. Ji, H. Jeong, M. Bakhtiary-Noodeh, S.-C. Shen, T. Detchprohm, A. K. Sood, P. Ghuman, S. Babu, N. K. Dhar, J. Lewis, and R. D. Dupuis, "Demonstration of uniform and reliable GaN p-i-p-i-n separate-absorption-and-multiplication ultraviolet avalanche photodiode arrays with large detection area," Proc. SPIE 10918, 1091814 (2019).

[10] A. K. Sood, J. W. Zeller, P. Ghuman, S. Babu, R. D. Dupuis, and H. Efstathiadis, "Development of high performance ultraviolet and near-infrared detector technologies." Proc. SPIE 10766, 1076609 (2018).

[11] A. K. Sood, J. W. Zeller, P. Ghuman, S. Babu, and R. D. Dupuis. "High performance GaN/AlGaN ultraviolet avalanche photodiode detector technologies." Proc. SPIE 10980, 109800M (2019).